(*12*). Irradiated mice suffer extensive microvascular endothelial cell death in the small intestine (*20*) (Fig. 4B); therefore irradiation is a means of both replacing the hematopoietic compartment and stimulating intestinal vascular repair and growth in wild-type mice. Transplantation with SLP-76–deficient but not wild-type marrow resulted in a loss of normal blood vessel architecture in the intestine as well as blood-filled mesenteric lymphatics, phenocopying the vascular phenotype of SLP-76–deficient animals (compare Fig. 4, C and D, with Fig. 2A). These results demonstrate that loss of SLP-76 or Syk exclusively in hematopoietic cells is sufficient to confer the angiogenic phenotype.

Recent angiogenic studies have indicated that a subset of endothelial precursor cells may be derived from the bone marrow (*21–24*). Thus, conferral of the angiogenic phenotype by SLP-76–deficient and Syk-deficient marrow could be due to a cell-autonomous defect in bone marrow–derived endothelial cell precursors. To address this possibility, we performed 5-bromo-4-chloro-3-indolyl β-D-galactopyranoside (X-gal) staining of the intestines of animals that received Tie2-LacZ$^{+}$, *slp-76*$^{-/-}$ marrow to identify donor-derived endothelial cells. X-gal staining revealed a considerable number of positive circulating cells [consistent with previous studies with the Tie2 promoter (*25*)] but only a single positive endothelial cell (fig. S2). This result is consistent with functional complementation experiments in which the mixing of small amounts of wild-type marrow (<10%) with SLP-76–deficient or Syk-deficient bone marrow completely rescued development of the vascular phenotype (*14, 26*). These results support a non–cell-autonomous mechanism in which SLP-76 and Syk signals are required in circulating cells to regulate separation of blood and lymphatic vascular networks. Further analysis of SLP-76/Syk signaling will shed light on the mechanisms by which hematopoietic signals influence vascular growth and development.


**References and Notes**

1. G. Oliver, M. Detmar, *Genes Dev.* **16**, 773 (2002).
2. K. Alitalo, P. Carmeliet, *Cancer Cell* **1**, 219 (2002).
3. F. Sabin, *Am. J. Anat.* **4**, 367 (1901).
4. J. T. Wigle, G. Oliver, *Cell* **98**, 769 (1999).
5. D. J. Dumont *et al.*, *Science* **282**, 946 (1998).
6. N. Gale *et al.*, *Dev. Cell* **3**, 411 (2002).
7. M. Turner *et al.*, *Nature* **378**, 298 (1995).
8. A. M. Cheng *et al.*, *Nature* **378**, 303 (1995).
9. J. L. Clements *et al.*, *J. Clin. Invest.* **103**, 19 (1999).
10. V. Pivniouk *et al.*, *Cell* **94**, 229 (1998).
11. D. Wang *et al.*, *Immunity* **13**, 25 (2000).
12. Materials and methods are available as supporting material on *Science* Online.
13. E. Braunwald, *Heart Disease* (Saunders, Philadelphia, 1997).
14. F. Abtahian *et al.*, unpublished observations.
15. A. Kaipainen *et al.*, *Proc. Natl. Acad. Sci. U.S.A.* **92**, 3566 (1995).
16. R. Prevo, S. Banerji, D. J. Ferguson, S. Clasper, D. G. Jackson, *J. Biol. Chem.* **276**, 19420 (2001).
17. E. Kriehuber *et al.*, *J. Exp. Med.* **194**, 797 (2001).
18. B. Sauter, D. Foedinger, B. Sterniczky, K. Wolff, K. Rappersberger, *J. Histochem. Cytochem.* **46**, 165 (1998).
19. J. T. Wigle *et al.*, *EMBO J.* **21**, 1505 (2002).
20. F. Paris *et al.*, *Science* **293**, 293 (2001).
21. T. Takahashi *et al.*, *Nature Med.* **5**, 434 (1999).
22. D. Lyden *et al.*, *Nature* **401**, 670 (1999).
23. D. Lyden *et al.*, *Nature Med.* **7**, 1194 (2001).
24. P. Carmeliet, A. Luttun, *Thromb. Haemost.* **86**, 289 (2001).
25. Y. Y. Kisanuki *et al.*, *Dev. Biol.* **230**, 230 (2001).
26. B. A. Judd *et al.*, *Proc. Natl. Acad. Sci. U.S.A.* **97**, 12056 (2000).


27. We thank E. Morrisey for thoughtful discussions; S. Millar, S. Reddy, and Y. Q. Jiang for assistance with in situ hybridization; J. Clements for critical reagents; S. Pickup for technical assistance; and S. Millar, C. Thompson, C. Simon, S. Reiner, and J. Epstein for critical reading of the manuscript.


**Supporting Online Material**

www.sciencemag.org/cgi/content/full/299/5604/247/DC1
Materials and Methods
Figs. S1 and S2
Movies S1 to S4


16 October 2002; accepted 19 November 2002


# KCNQ1 Gain-of-Function Mutation in Familial Atrial Fibrillation


**Yi-Han Chen,[1]*† Shi-Jie Xu,[2,3]*† Saïd Bendahhou,[4] Xiao-Liang Wang,[5] Ying Wang,[2] Wen-Yuan Xu,[1] Hong-Wei Jin,[5] Hao Sun,[2] Xiao-Yan Su,[1] Qi-Nan Zhuang,[2] Yi-Qing Yang,[1] Yue-Bin Li,[2] Yi Liu,[1] Hong-Ju Xu,[1] Xiao-Fei Li,[1] Ning Ma,[1] Chun-Ping Mou,[1] Zhu Chen,[2,6] Jacques Barhanin,[4] Wei Huang[2,3,6]**



**Atrial fibrillation (AF) is a common cardiac arrhythmia whose molecular etiology is poorly understood. We studied a family with hereditary persistent AF and identified the causative mutation (S140G) in the *KCNQ1* (*KvLQT1*) gene on chromosome 11p15.5. The *KCNQ1* gene encodes the pore-forming α subunit of the cardiac $I_{Ks}$ channel (KCNQ1/KCNE1), the KCNQ1/KCNE2 and the KCNQ1/KCNE3 potassium channels. Functional analysis of the S140G mutant revealed a gain-of-function effect on the KCNQ1/KCNE1 and the KCNQ1/KCNE2 currents, which contrasts with the dominant negative or loss-of-function effects of the KCNQ1 mutations previously identified in patients with long QT syndrome. Thus, the S140G mutation is likely to initiate and maintain AF by reducing action potential duration and effective refractory period in atrial myocytes.**


Atrial fibrillation is characterized by rapid and irregular activation of the atrium. The prevalence of AF in the general population rises with increasing age, ranging from <1% in young adults to >5% in those older than 65 years (*1*). AF causes thromboembolism, tachycardia-mediated cardiomyopathy, heart failure, and ventricular arrhythmia (*2*) and is a considerable financial burden on the health-care system (*3*). The ionic properties of the atria play an important role in determining the occurrence and properties of atrial arrhythmias; sustained AF is associated with atrial electrical remodeling. Both a decrease of the L-type calcium current ($I_{Ca,\ L}$) and an increase of $I_{K1}$ and $I_{KAch}$ $K^+$ currents have been considered important factors in AF initiation and maintenance (*4*). Atrial fibrillation can occur on a familial basis, pointing to a genetic cause of the arrhythmia in some individuals. Hereditary AF in three families was recently linked to a locus between D10S1694 and D10S1786 on chromosome 10 (*5*).

We studied a four-generation family with autosomal dominant hereditary AF from Shandong Province, People's Republic of China. The proband (II-14, Fig. 1) was identified 23 years ago at the age of 22; 16 affected members were alive in the family at the time of this study.


[1]Department of Cardiology, Tongji Hospital, and Institute of Medical Genetics, Tongji University, 399 Xin Cun Road, Shanghai 200065, People's Republic of China. [2]Chinese National Human Genome Center at Shanghai, 250 Bi Bo Road, Shanghai 201203, People's Republic of China. [3]Health Science Center, Institute for Biological Sciences–Chinese Academy of Sciences and Shanghai Second Medical University, Shanghai 200025, People's Republic of China. [4]Institut de Pharmacologie Moléculaire et Cellulaire, CNRS, 660 Route des lucioles, 06560 Sophia Antipolis, France. [5]Institute of Materia Media, Chinese Academy of Medical Sciences, 1 Xian Nong Tan Street, Beijing 100050, People's Republic of China. [6]State Key Laboratory of Medical Genomics, Shanghai Institute of Hematology, Rui Jin Hospital affiliated to Shanghai Second Medical University, Shanghai 200025, People's Republic of China.

*These authors contributed equally to this work.
†To whom correspondence should be addressed. E-mail: drchen@public7.sta.net.cn (Y.-H.C.); xusj@chgc.sh.cn (S.-J. X.)

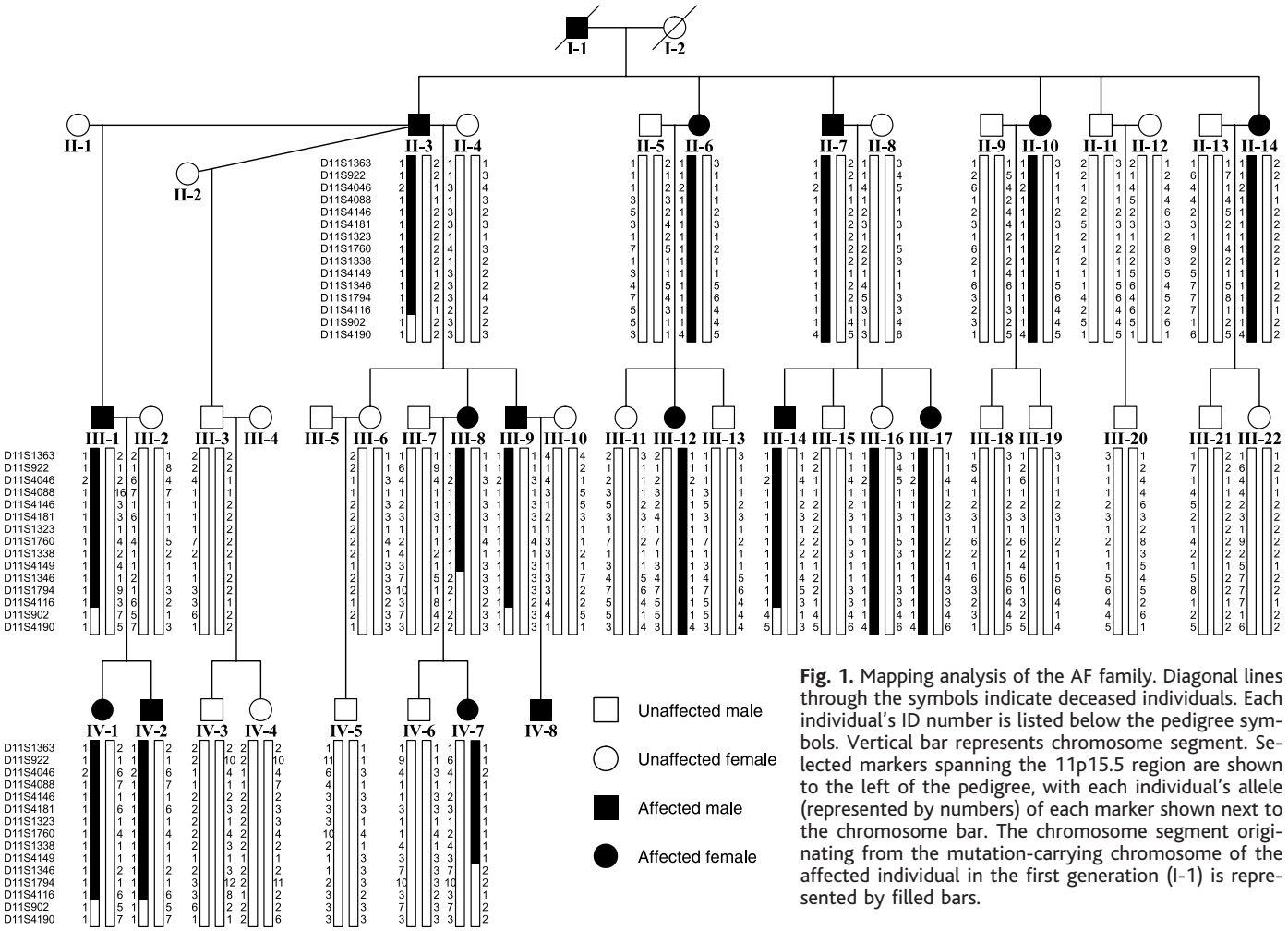


**Fig. 1.** Mapping analysis of the AF family. Diagonal lines through the symbols indicate deceased individuals. Each individual's ID number is listed below the pedigree symbols. Vertical bar represents chromosome segment. Selected markers spanning the 11p15.5 region are shown to the left of the pedigree, with each individual's allele (represented by numbers) of each marker shown next to the chromosome bar. The chromosome segment originating from the mutation-carrying chromosome of the affected individual in the first generation (I-1) is represented by filled bars.

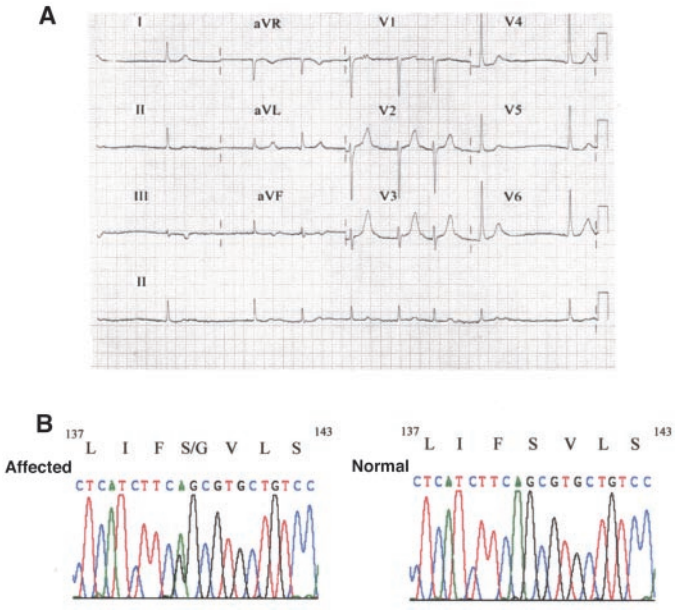


**Fig. 2.** S140G mutation in *KCNQ1* is associated with atrial fibrillation. (**A**) Twelve-lead ECG of an affected individual (III-9). (**B**) DNA and amino acid sequence of KCNQ1 missense mutation associated with affected members in the AF family. DNA sequence analysis revealed an A to G substitution causing an S140G mutation in the S1 segment of KCNQ1.

AF persisted in affected individuals once it appeared (Fig. 2A). After eliminating structural heart disease or systemic diseases as the cause of AF in the family, we performed microsatellite whole-genome screening. Linkage analysis gave a maximum LOD score (logarithm of the odds ratio for linkage) at zero recombination of 4.55 at D11S4181, with other flanking markers also supporting the linkage. Further haplotype examination narrowed the AF locus to a critical region about 19.6 cM (~12 Mb) between D11S1363 and D11S1346 on 11p15.5 (Fig. 1).

One obvious candidate gene in the critical region was *KCNQ1*. This gene encodes a potassium channel subunit associated with long QT (LQT) syndrome, a cardiac disorder characterized by prolonged QT interval on electrocardiogram (ECG), syncope, and sudden cardiac death due to ventricular tachyarrhythmia (*6*). Sequence analysis of the *KCNQ1* coding region revealed a missense mutation S140G (A to G substitution at nucleotide 418) in all of the affected family members (Fig. 2B). This mutation was not observed in normal individuals in the AF family with the exception of individual III-16, probably due to delayed manifestation or incomplete phenotype penetrance (Fig. 1, table S1). Furthermore, this mutation was absent in 188 healthy control individuals. Serine 140 is well conserved among different species and is located in the S1 transmembrane segment of KCNQ1 in a position close to the extracellular surface of the plasma membrane. Interestingly, no LQT-associated mutation is located in the S1 segment of the KCNQ1 (*7*).

Because mutations in *KCNQ1* have been

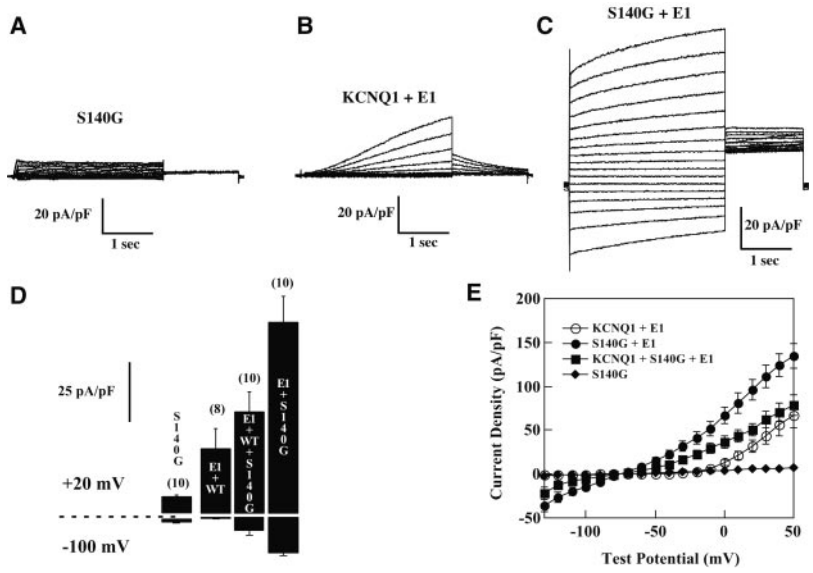


**Fig. 3.** The S140G mutation alters the KCNQ1-KCNE1 current. (**A**) Representative current traces recorded from COS-7 cells transfected with the S140G mutant alone, (**B**) with wild-type (WT) KCNQ1 and KCNE1, and (**C**) with S140G-KCNQ1 and KCNE1. (**D**) Comparison of current density at −100 mV (inward current) and +20 mV (outward current) for cells transfected with 0.75 μg of S140G mutant cDNA alone, or 0.75 μg of KCNQ1 (WT) and 0.25 μg of KCNE1, or 0.375 μg of KCNQ1 (WT) and 0.375 μg of S140G with 0.25 μg of KCNE1, or 0.75 μg of S140G mutant and 0.25 μg of KCNE1. (**E**) Current density is plotted versus voltage for the indicated transfection combination. Cells were held at −80 mV before depolarization to various potentials ranging from −130 mV to +50 mV in a 10-mV increment for 3 s, then held at −40 mV for 1.5 s. The number of cells is shown in parentheses. Values represent means ± SEM.

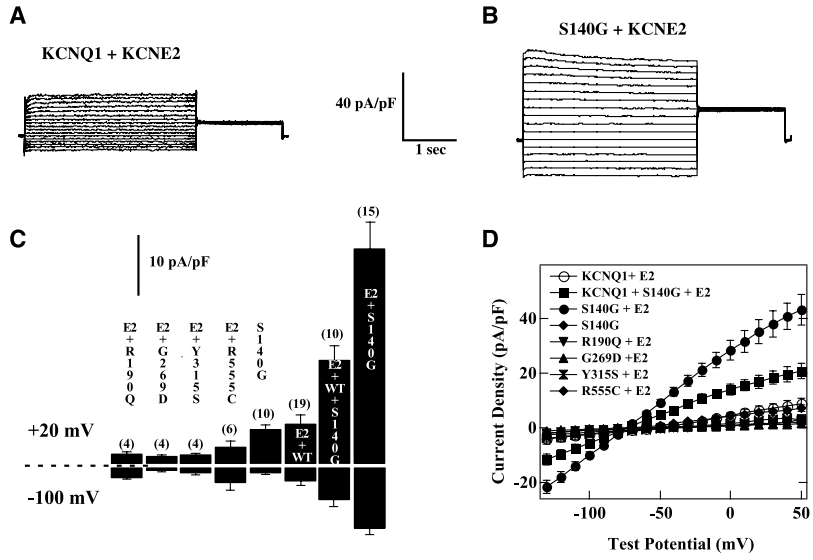


**Fig. 4.** The S140G mutation alters the KCNQ1−KCNE2 current. (**A**) Current traces from COS-7 cells cotransfected with KCNQ1 and KCNE2 or (**B**) with S140G and KCNE2. (**C**) Current density at −100 mV (inward current) and +20 mV (outward current) from transiently transfected COS-7 cells with equivalent amounts of cDNA as described in Fig. 3 for KCNQ1 and KCNE1 clones. (**D**) Current density is plotted versus voltage for the indicated transfectants as in Fig. 3E. The number of cells is shown in parentheses. Values represent means ± SEM.

associated with LQT syndrome, we measured the mean corrected QT interval (QTc) for the affected members (table S1). Intriguingly, some affected individuals displayed prolonged QTc (9 of 16 patients, range 0.45 to 0.53 s) (*8*). However, a previous study on QT interval suggested that AF was associated with prolongation of the mean QT interval (28 of 50 patients) (*9*). Indeed, our own ECG data from sporadic AF patients also confirmed that many of them have prolonged QTc values (10 of 25 patients with idiopathic AF, range 0.45 to 0.52 s; 87 of 197 patients with acquired AF, range 0.45 to 0.57 s) (*10*). Sudden cardiac death did not occur in this family. The near-syncope and syncope incidents that occurred in the two affected members of the family were probably caused by bradycardia and transient ischemic attacks as a result of thromboembolism in AF. It is not clear whether part of the prolonged QT interval is attributable to secondary effects of AF (e.g., heart muscle disease); the value of the QT interval does not appear to correlate with AF persistent time (table S1).

KCNQ1 associates with small subunits from the KCNE family (KCNE1 to KCNE4) (*11*–*15*). In cardiac myocytes, KCNQ1 associates with KCNE1 to form the $I_{Ks}$ current (*11*, *12*). To identify a mechanism for the AF phenotype and confirm that the S140G substitution is not a benign polymorphism, we expressed the S140G mutant in COS-7 cells and assessed the channel function by whole-cell patch-clamping. Expression of the S140G mutant alone did not produce a substantial current (5.5 ± 0.8 pA/pF at +20 mV) (Fig. 3A). When the S140G mutant was coexpressed with KCNE1, however, the current density was markedly enhanced at all voltages (Fig. 3, B and C). At +20 mV, current density was increased by a factor of 3 (95.5 ± 12.1 pA/pF for S140G mutant–KCNE1 versus 32.2 ± 7.2 pA/pF for wild-type KCNQ1-KCNE1) (Fig. 3D). In addition, the S140G mutation drastically modified the gating and kinetic properties, leading to currents with an apparently instantaneous activation and deactivation and a linear current-voltage relation (Fig. 3, C and E).

KCNQ1 can also form functional potassium channels with KCNE2 and KCNE3 (*13*, *14*), which are both expressed in human atrium and ventricle (fig. S1). Coexpression of KCNQ1 and KCNE2 induced a sixfold increase in current density (35.5 ± 4.3 pA/pF for S140G mutant–KCNE2 versus 6.5 ± 1.5 pA/pF for wild-type KCNQ1-KCNE2 at +20 mV) (Fig. 4, A to C). However, there was no difference observed in current density when KCNE3 was used for cotransfection (27.7 ± 7.2 pA/pF for wild-type KCNQ1-KCNE3 versus 28.7 ± 6.1 pA/pF for S140G mutant–KCNE3 at +20 mV) (*10*). Currents produced by the S140G mutant–KCNE1, –KCNE2, and –KCNE3 combinations were all abolished after bath application of 10 μM KCNQ1 inhibitor *trans*-6-cyano4-(*N*-ethylsulfonyl-*N*-methylamino)-3-hydroxy-2,2-dimethyl-chromanane (Chromanol 293B). Furthermore, coexpression of the KCNE2 and LQT-associated KCNQ1 mutations (R190Q, G269D, Y315S, and R555C) produced a loss-of-function channel, showing that current enhancement was specifically associated with the S140G mutation (Fig. 4, C and D).

Thus, in contrast to the LQT-associated mutations in KCNQ1, which all have a dominant negative effect (*16*, *17*), the AF-associated KCNQ1 mutation leads to a gain of potassium channel function.

Animal studies and clinical data have indicated that AF is caused mainly by multiple-

circuit-reentry, which is facilitated by shortening of action potential duration (APD) and reduction of effective refractory period (ERP) (*4*). In this study, when coexpressed with KCNE1 and KCNE2, the S140G mutation caused a substantial increase of inward potassium current at hyperpolarized potential. This would stabilize the resting membrane potential, leading to a shortening of the atrial ERP. Coexpression of the S140G mutant with KCNE1 and KCNE2 also led to an increase in the outward current at depolarized potential, which is expected to shorten the repolarization phase of the atrial action potential. Thus, both of these alterations provide a good substrate for AF.

Given that $I_{Ks}$ and KCNQ1-KCNE2 are expressed in both atrium and ventricle, it is surprising that the QTc values were not reduced in our patients. However, the duration of the QT interval depends not only on the prevailing heart rate but also on the instantaneous interval between beats. Thus, a simple correction of QT interval for heart rate in AF is inadequate (*9, 18*). The failure to detect shortening of the QT interval may be due to irregular ventricular beats, which can skew the accurate representation of QT interval on the ECG of AF patients. Alternatively, a stronger compensation for $I_{Ks}$ and/or KCNQ1-KCNE2 enhancement may take place in the ventricle as compared with the atrium because of the different repertoire of ion channels in the two heart chambers. An arrhythmia-induced electrical remodeling may be responsible for such a difference. Further studies with an S140G animal model or with gene expression profiling may shed more light on the molecular determinants of AF (*19*). Finally, we cannot rule out the possibility that another mutation in a yet unidentified gene in the same critical region also contributes to the phenotype.

Familial AF is likely to be genetically heterogeneous. We did not detect mutations in *KCNQ1* in AF patients from six additional small hereditary AF families and 19 sporadic idiopathic AF patients, and another AF locus has already been mapped to chromosome 10 (*5*).

Although calcium overload and changes in calcium channels are believed to be important in the initiation and maintenance of AF (*4*), our study indicates that an increased current in $I_{Ks}$ and/or KCNQ1-KCNE2 channels can also lead to AF by shortening atrial APD and ERP. This is supported by a recent genetic study linking a variant of KCNE1 with an increased risk for AF (*20*). Our findings demonstrate how the diverse functional behavior of a single ion channel can evoke distinct cardiac disorders, as exemplified by *SCN5A (21–23)*, a sodium channel gene whose mutations have been associated with LQT syndrome, Brugada syndrome, and cardiac conduction disease. Finally, the unexpected role of KCNQ1 in generating AF suggests that $I_{Ks}$ blockers may offer therapeutic benefit for a subset of patients with AF.


**References and Notes**

1. W. M. Feinberg, J. L. Blackshear, A. Laupacis, R. Kronmal, R. G. Hart, *Arch. Intern. Med.* **155**, 469 (1995).
2. S. S. Chugh, J. L. Blackshear, W. K. Shen, S. C. Hammill, B. J. Gersh, *J. Am. Coll. Cardiol.* **37**, 371 (2001).
3. D. S. Cannom, *Am. J. Cardiol.* **85**, 25D (2000).
4. S. Nattel, *Nature* **415**, 219 (2002).
5. R. Brugada *et al., N. Engl. J. Med.* **336**, 905 (1997).
6. Q. Wang *et al.*, *Nature Genet.* **12**, 17 (1996).
7. M. T. Keating, M. C. Sanguinetti, *Cell* **104**, 569 (2001).
8. Materials and methods are available as supporting material on *Science* Online.
9. G. R. Pai, J. M. Rawles, *Br. Heart J.* **61**, 510 (1989).
10. Data are available from the authors upon request.
11. J. Barhanin *et al.*, *Nature* **384**, 78 (1996).
12. M. C. Sanguinetti *et al.*, *Nature* **384**, 81 (1996).
13. N. Tinel, S. Diochot, M. Borsotto, M. Lazdunski, J. Barhanin, *EMBO J.* **19**, 6326 (2000).
14. B. C. Schroeder *et al.*, *Nature* **403**, 196 (2000).
15. M. Grunnet *et al., J. Physiol.* **542**, 119 (2002).
16. C. Chouabe *et al., EMBO J.* **16**, 5472 (1997).
17. Z. Wang *et al., J. Cardiovasc. Electrophysiol.* **10**, 817 (1999).
18. W. A. Seed *et al.*, *Br. Heart J.* **57**, 32 (1987).
19. R. Mazhari, H. B. Nuss, A. A. Armoundas, R. L. Winslow, E. Marban, *J. Clin. Invest.* **109**, 1083 (2002).
20. L. P. Lai *et al., Am. Heart J.* **144**, 485 (2002).
21. Q. Wang *et al.*, *Cell* **80**, 805 (1995).
22. Q. Chen *et al.*, *Nature* **392**, 293 (1998).
23. H. L. Tan *et al.*, *Nature* **409**, 1043 (2001).



24. We thank P.-L. Xie for helpful comments on this work, W.-Q. Liu and Y. Zhao for assistance with linkage analysis, G. Romey for assistance with the electrophysiological study, and the AF family members for their participation. Supported by grants from the National Natural Science Foundation (3993420, 39900060, and 30170386), Chinese High Tech Program, the National Key Program on Basic Research (G1998051002), Foundation for University Key Teacher by the Ministry of Education (1508-110001), the Shanghai Science and Technology Development Fund (00DJ14003, 99ZB14024), fund from Shanghai Commission for Education, CNRS, and the Fondation pour la Recherche Médicale and the Association Française contre les Myopathies (S.B.). This study was approved by the ethics committee of Chinese Human Genome Center at Shanghai.


**Supporting Online Material**

www.sciencemag.org/cgi/content/full/299/5604/251/DC1
Materials and Methods
Fig. S1
Table S1
References

27 August 2002; accepted 4 November 2002

# Ringlike Structure of the *Deinococcus radiodurans* Genome: A Key to Radioresistance?

**Smadar Levin-Zaidman,[1] Joseph Englander,[1] Eyal Shimoni,[1] Ajay K. Sharma,[2] Kenneth W. Minton,[3] Abraham Minsky[1]***

**The bacterium *Deinococcus radiodurans* survives ionizing irradiation and other DNA-damaging assaults at doses that are lethal to all other organisms. How *D. radiodurans* accurately reconstructs its genome from hundreds of radiation-generated fragments in the absence of an intact template is unknown. Here we show that the *D. radiodurans* genome assumes an unusual toroidal morphology that may contribute to its radioresistance. We propose that, because of restricted diffusion within the tightly packed and laterally ordered DNA toroids, radiation-generated free DNA ends are held together, which may facilitate template-independent yet error-free joining of DNA breaks.**

*Deinococcus radiodurans* is capable of surviving 15,000 grays (Gy) of ionizing radiation, whereas doses below 10 Gy are lethal to all other organisms (*1*, *2*). The bacterium's phenomenal radioresistance derives from its ability to accurately mend hundreds of double-strand DNA breaks (*2–7*). This mending is unlikely to occur by homologous recombination, the only known mechanism for high-fidelity repair of double-strand breaks, because this mechanism is ineffective when chromosomes are extensively shattered. The enigmatic nature of *D. radiodurans*' radioresistance is highlighted by the finding that this organism encodes a typical bacterial complement of DNA repair enzymes (*7–9*).

To investigate the factors responsible for the radioresistance of *D. radiodurans,* we studied the morphology of the bacterium. Our scanning electron microscopy analysis (*10*) confirmed previous observations (*11*) that each *D. radiodurans* cell has two perpendicular furrows that result in a tetrad morphology. This morphology is exhibited by all cells in a stationary state and by >90% of actively growing cells (fig. S1A). Differential interference contrast and fluorescence microscopy (fig. S1, B to D), as well as integrated fluorescence intensity measurements (*10*), revealed that in stationary-state bacteria, the four compartments contain an equal amount of DNA. Uniform compartmentalization of DNA was also de-

[1]Department of Organic Chemistry, The Weizmann Institute of Science, Rehovot 76100, Israel. [2]Laboratory of Molecular Pharmacology, National Cancer Institute/National Institutes of Health, Bethesda, MD 20892, USA. [3]Department of Pathology, Uniformed Services University of the Health Sciences, Bethesda, MD 20814–4799, USA.

*To whom correspondence should be addressed. E-mail: avi.minsky@weizmann.ac.il